Electronic Supplementary Material (ESI) for Chemical Science.


| | **αHer2/XTEN-May$_{16}$** | **αHer2/XTEN** | **αHer2** | **αHer2/May$_2$** |
|---|---|---|---|---|
| $C_{max}$ (ug/mL) | 125 ± 3.84 | 115 ± 6.74 | 98.0 ± 3.47 | 90.3 ± 8.80 |
| $AUC_{0-28}$ (day•ug/mL) | 570 ± 18.0 | 776 ± 24.0 | 765 ± 25.5 | 663 ± 38.4 |
| $AUC_{0-inf}$ (day•ug/mL) | 685 | 897 | 1090 | 822 |
| CL (mL/day/kg) | 7.30 | 5.57 | 4.61 | 6.08 |
| Vss (mL/kg) | 102 | 72.8 | 103 | 104 |
| $T_{1/2}$ (day) | 10.0 | 8.96 | 15.3 | 12.2 |

**Supplementary Table 1**. Pharmacokinetic parameters for high-DAR maytansinoid TXC **(αHer2/XTEN-May$_{16}$)** versus XTENylated antibody lacking payloads (**αHer2/XTEN**), low-DAR TDC (**αHer2/May2**), and THIOMAB antibody control (**αHer2**).

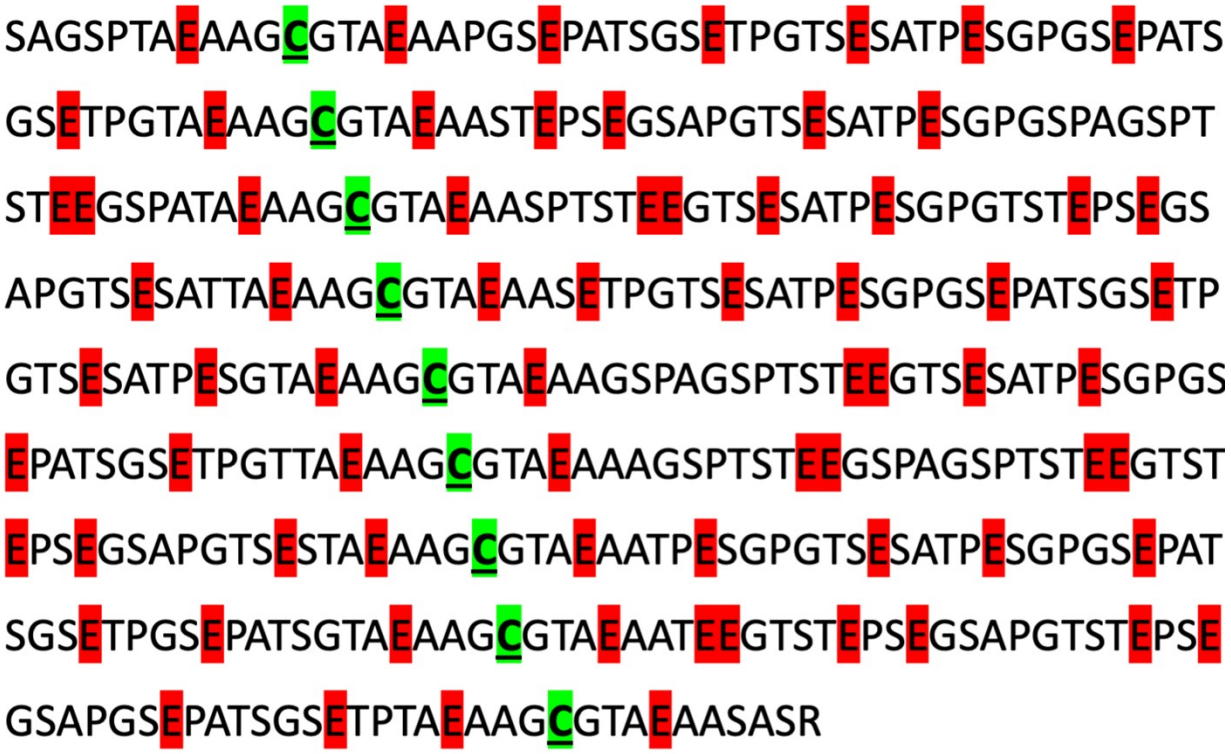


**Supplementary Figure 1.** Sequence of 432-amino acid XTEN with 9 cysteines (green) used for conjugation and generation of TXCs **αCD22/XTEN-May$_{16}$**, **αHer2/XTEN-May$_{16}$** and **αCD22/XTEN-PBD*ma*$_{18}$**. For reference, this XTEN contains 71 glutamic acid residues, or 16% of the sequence (red).

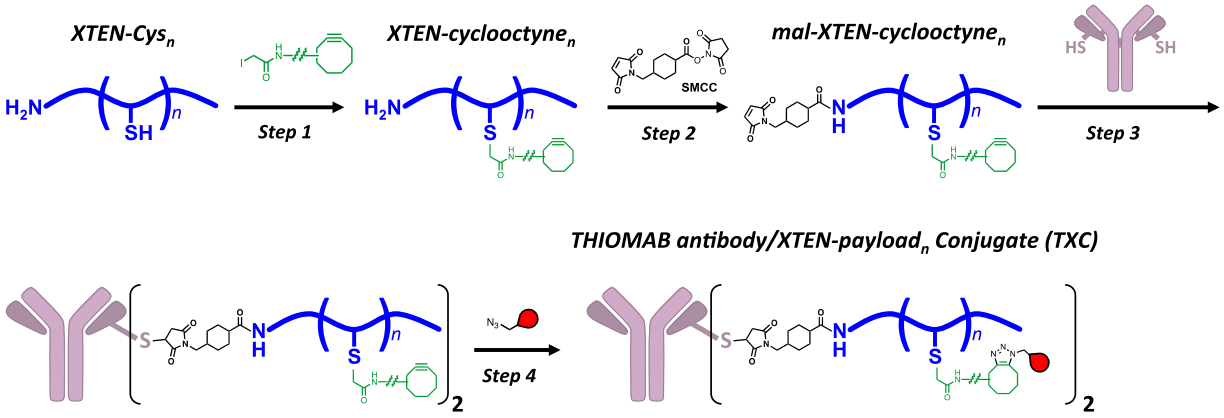


**Supplementary Figure 2.** Click chemistry-based conjugation strategy to generate TXCs involving (Step 1) conjugation of a cyclooctyne-containing molecule to *n* engineered Cys of XTEN, (Step 2) reaction of the XTEN N-terminus with SMCC to install a maleimide, (Step 3) reaction with engineered Cys of a THIOMAB antibody, and (Step 4) strain-promoted click chemistry reaction of the cyclooctynes with an azide-bearing payload.

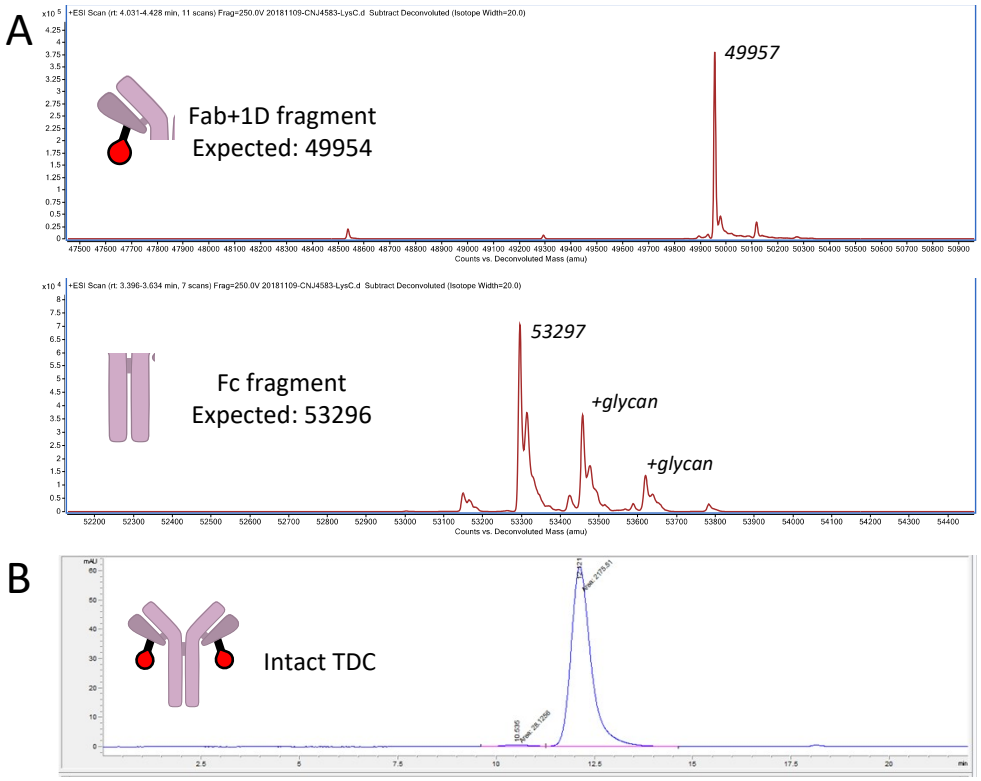


**Supplementary Figure 3.** Analysis of **αCD22/PBD*ma*$_2$** TDC by (A) middle-down LC/MS and (B) analytical size-exclusion chromatography. To increase mass spectrometry sensitivity the TDC was partially digested by LysC to generate Fab and Fc fragments for LC/MS analysis.

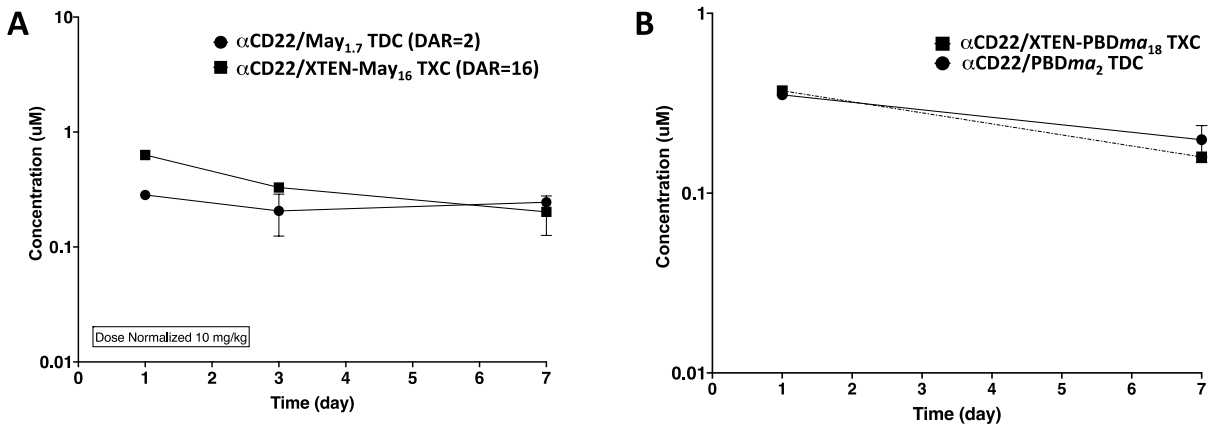


**Supplementary Figure 4.** Dose-normalized sparse pharmacokinetic analysis of total circulating antibody conjugate isolated from the mouse xenograft experiments for TXCs and TDCs with (A) maytansinoid or (B) PBD*ma* payloads, shown in Figure 6.

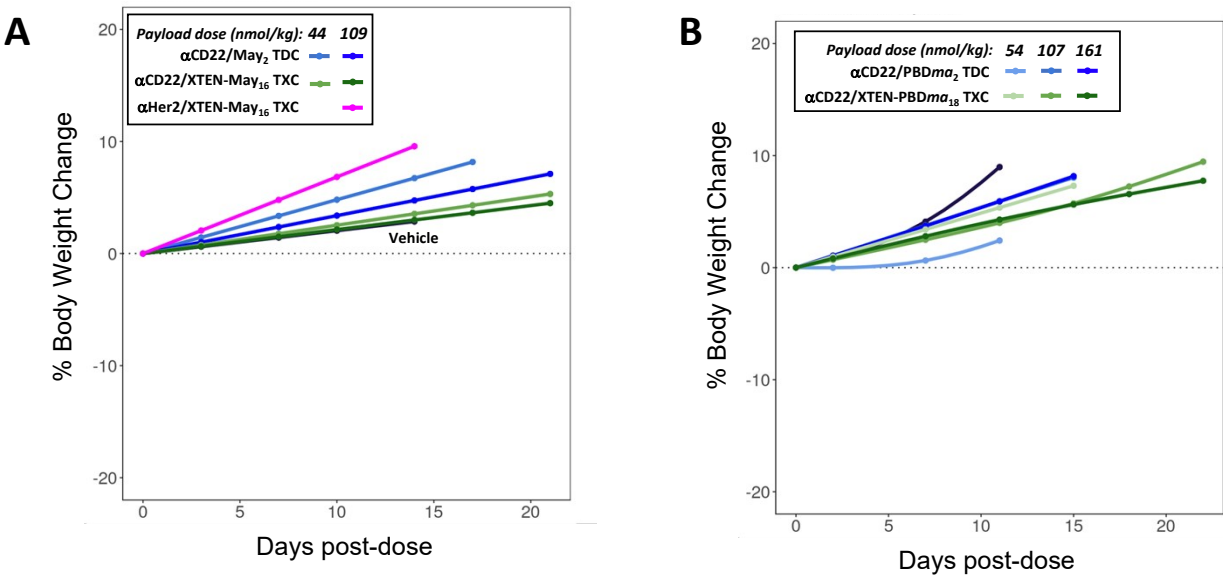


**Supplementary Figure 5.** Tolerability, measured as %body weight change, for anti-CD22 TXCs and TDCs with (A) maytansinoid payload or (B) PBD*ma* payload from mouse xenograft experiment shown in Figure 6. Cubic spline fitted body weight changes relative to day 0 baseline are plotted for each treatment group (n=5/group) over the duration of study.

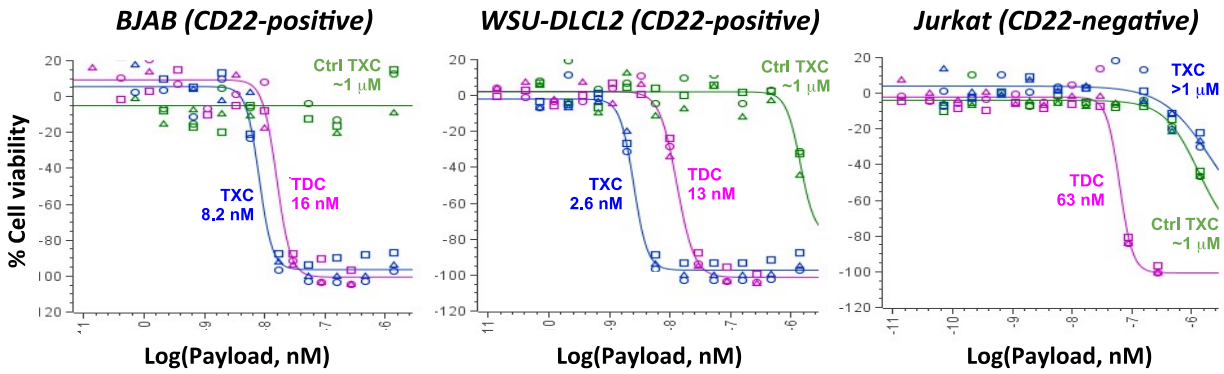


**Supplementary Figure 6.** In vitro potency of **αCD22/XTEN-May$_{16}$** TXC (DAR=16), **αCD22/May$_{1.7}$** TDC (DAR=2) and control **αHer2/XTEN-May$_{16}$** TXC (DAR=16) against BJAB (CD22-positive), WSU-DLCL2 (CD22-positive) and Jurkat cells (CD22-negative). $IC_{50}$ values (payload concentration) are displayed.

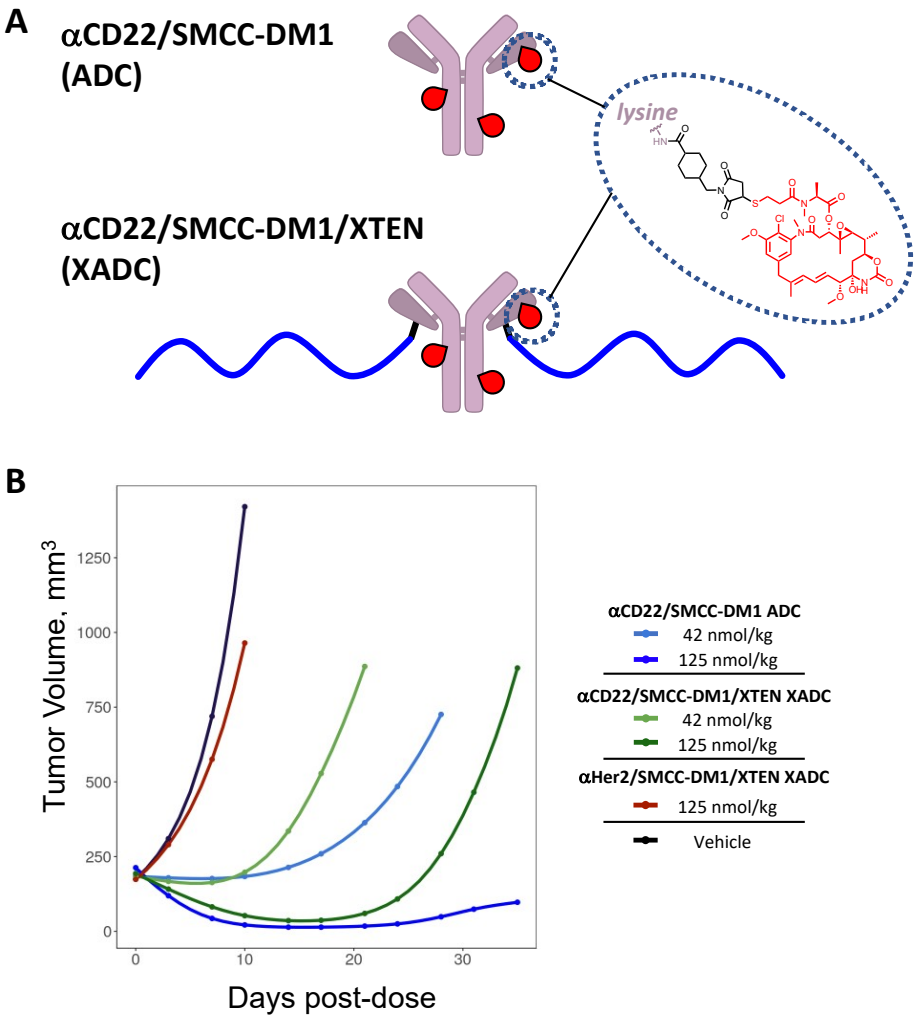


**Supplementary Figure 7.** Impact of XTEN on ADC in vivo efficacy. (A) Structures of XTENylated ADC (XADC) and parent ADC, both targeting CD22 and bearing the same number of SMCC-DM1 on antibody lysine residues (4.5). (B) In vivo efficacy comparison of ADC and XADC in BJAB tumor xenograft model at matched payload dose levels of 42 and 125 nmol/kg. SCID mice bearing subcutaneous tumors (~200 $mm^3$) received a single intravenous injection of vehicle or conjugate on day 0. Cubic spline fitted tumor volumes are plotted for each treatment group (n=8/group) over the duration of study.

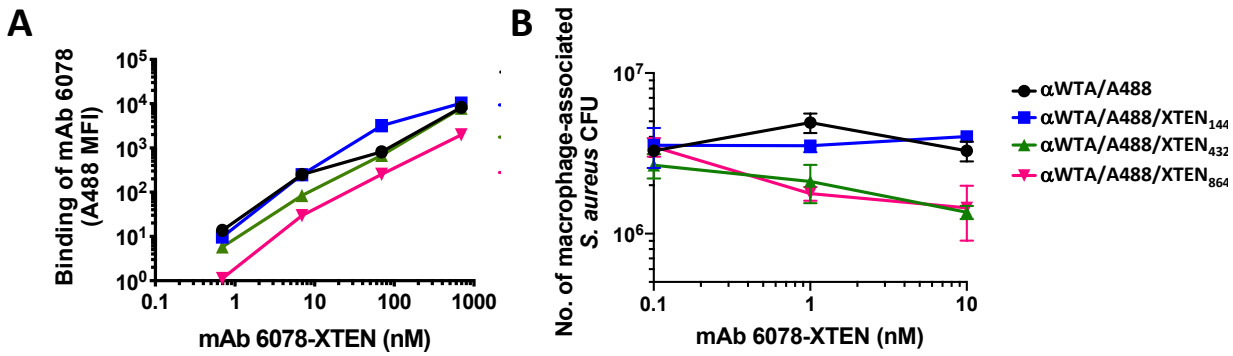


**Supplementary Figure 8.** Short $XTEN_{144}$ peptide (144 amino acids) does not affect binding of mAb to *S. aureus* bacteria and association of opsonized *S. aureus* with phagocytes. (A) Binding of αWTA/A488 (no XTEN) or of Alexa488-labeled αWTA XADCs with XTEN peptides of different lengths ($XTEN_{144}$=144 amino acids, $XTEN_{432}$=432 amino acids, $XTEN_{864}$=864 amino acids) to *S. aureus*, as assessed by flow cytometry. (B) Association of *S. aureus* bacteria opsonized with αWTA/A488 or XTEN conjugates with murine RAW264.7 macrophages.

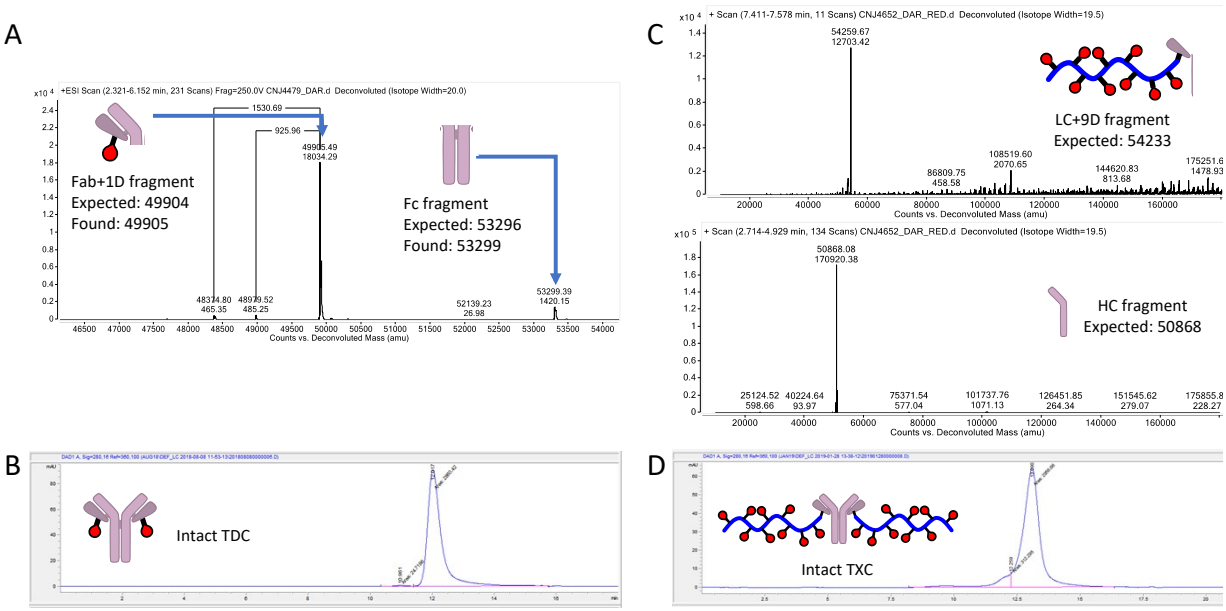


**Supplementary Figure 9.** Analysis of **αWTA/dmDNA31$_2$** TDC (DAR=2) and **αWTA/XTEN$_{144}$-dmDNA31$_{18}$** TXC (DAR=18) by (A and C) middle-down LCMS and (B and D) analytical size-exclusion chromatography. To increase mass spectrometry sensitivity the TDC was partially digested by LysC to generate Fab and Fc fragments and the TXC was partially reduced with DTT to generate light chain (LC) and heavy chain (HC) fragments; TDC and TXC fragments were analyzed in positive and negative ion mode, respectively. For SEC analysis, the TDC was injected on a TSKgel3000SW column and the TXC was injected onto a Yarra4000 column.

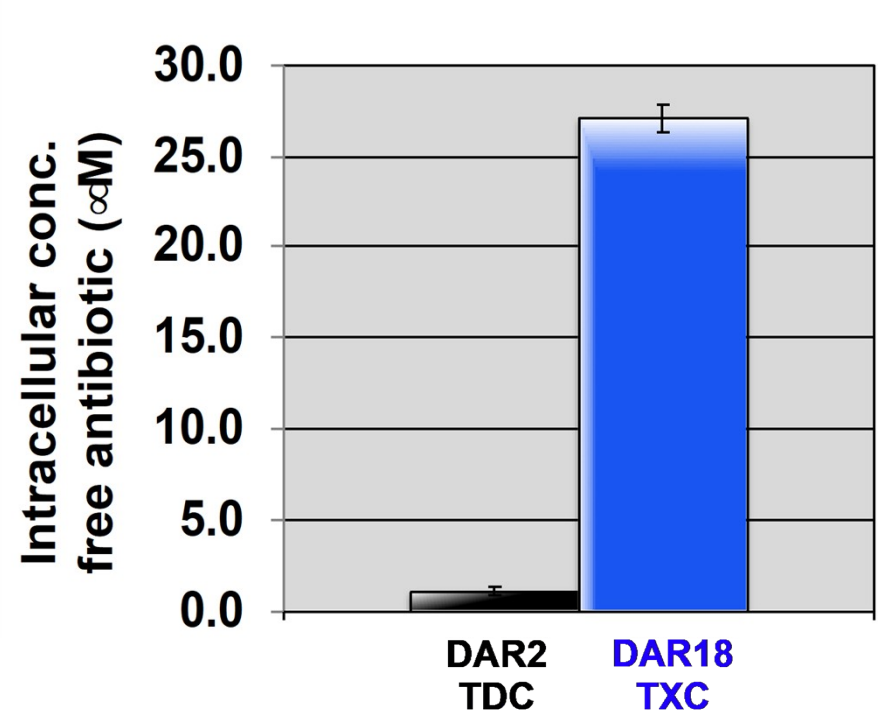


**Supplementary Figure 10.** High-DAR **αWTA/XTEN$_{144}$-dmDNA31$_{18}$** TXC (DAR=18) delivered a significantly higher intracellular concentration of released antibiotic dmDNA31 than the TDC **αWTA/dmDNA31$_2$**. *S. aureus* bacteria (USA300 strain) were pre-opsonized with an equimolar concentration of either conjugate (30 nM), added to macrophages to induce phagocytosis, and the macrophages were lysed to enable estimation of the intracellular concentration of dmDNA31 by LC/MS-MS. Data represent average ± standard deviation (n=3).

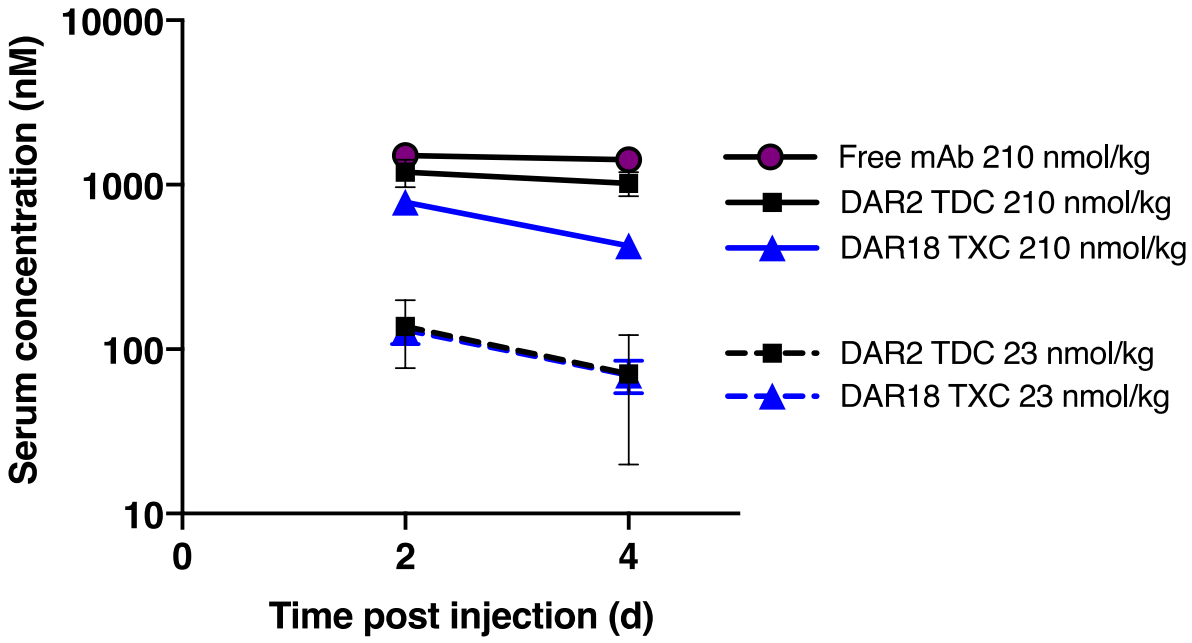


**Supplementary Figure 11.** Sparse pharmacokinetics of anti-*S. aureus* DAR18 TXC, DAR2 TDC, and free mAb in the *S. aureus* infection model. Mice were i.v. infected with *S. aureus,* and 1 day later i.v. injected with anti-*S. aureus* DAR18 TXC, DAR2 TDC, or free mAb (23 nmoles/kg or 210 nmoles/kg), as described in Figure 9. The serum concentration of DAR18 TXC at 2 and 4 d post injection, based on quantification of total antibody by using LC-MS/MS, was within approximately 2-fold that of free mAb or DAR2 TDC. Data are expressed as average ± SD of 5 (free mAb) or 7 (DAR18 TXC, DAR2 TDC) mice per group.